Steam gasification of cellulose pulp char: Insights on experimental and kinetic study with a focus on the role of Silicon

Majd Elsaddik, Ange Nzihou, Michel Delmas, Guo-Hua Delmas

Steam gasification of cellulose pulp char: Insights on experimental and kinetic study with a focus on the role of Silicon

Majd Elsaddik [a,*], Ange Nzihou [a,b,c], Michel Delmas [d], Guo-Hua Delmas [d]

[a] Université de Toulouse, Mines Albi, CNRS, Centre RAPSODEE, Campus Jarlard, F.81013 Albi Cedex 09, France
[b] School of Engineering and Applied Science, Princeton, NJ 08544, USA
[c] Princeton University, Andlinger Center for Energy and the Environment, Princeton, NJ 08544, USA
[d] BioEB, 6 Allee des Amazones, F-31320 Auzeville-Tolosane, France

This paper deals with steam gasification kinetics of cellulose pulp extracted from biomass with on the focus silicon effect. Isothermal TGA tests were performed under various operating conditions. The gasification reactivity increased with increasing temperature and steam pressures. The reactivity of cellulose pulp biochar was 3 times lower than that of the biomass char. This is attributed to the difference in the inorganic content, namely AAEM and Si. The gasification of pulp biochar revealed the negative effect of Si, which was the main inorganic element present in the cellulose pulp. Biochar reactivity decreased with increasing Si concentration. The reactivity could be correlated to Si content. The morphological structure had an impact at a low conversion rate, although it was less influential than Si. Thus, a kinetic model for describing the gasification kinetics was developed using %Si as a key-parameter. The comparison to the experimental data showed that the proposed model can reasonably predict the gasification behavior of different biochars with satisfactory accuracy (<10%) as far as industrial processes are concerned. Further analysis of alkaline-washed cellulose confirmed the inhibiting effect of Si on the gasification process. The reaction time was 2.5 times lower after the partial elimination of Si.

1. Introduction

According to the International Energy Agency outlook 2021, a 50% increase in energy consumption is expected by 2050, due to the population and economic growth [1]. It is reported that 79% of the total energy supply was provided by fossil fuels in 2020, down from 81% in 2010 [2]. However, fossil fuels are the largest source of carbon dioxide which is the principal greenhouse gas contributing to global warming. In the current energy context, lignocellulosic biomass has been regarded as a potential solution to address concerns about climate change and security of energy supply [3]. Lignocellulosic biomass is an abundant and economical renewable feedstock that represents roughly 50% of the biomass on earth.

Following a similar concept to crude oil refining, lignocellulosic biomass resources can be fractionated into their constituents that are further transformed by different routes into marketable renewable fuels and added-value chemicals. This concept of biorefinery is a strategic pillar to develop the circular economy. The *LeeBio*™ process (Low Extraction Energy of Biomass) allows lignocellulosic biomass to become a universal energy resource which can help to phase out reliance on fossil fuels [4]. This process is based on the chemical separation of lignocellulosic residues to cellulose, hemicelluloses and lignin. It is non-degradative and uses only formic acid (organosolv process) at atmospheric pressure. The profitability of this process is due to the fact that the extracted lignin and hemicelluloses can be introduced into industrial sectors without changing the existing technologies or infrastructures. In addition to its conventional applications, separated cellulose can be converted, like lignocellulosic biomass, into syngas through thermochemical conversion (Fig. 1).

Steam gasification is one of the main thermochemical conversion routes of lignocellulosic feedstocks to produce high quality syngas which can be used in different applications such as gas turbine combustion, SOFC (solid oxide fuel cell) operation and Fischer–Tropsch process. A solid material called biochar is also produced, Accounting up to 35% of biomass, biochar has wide range of physico-chemical properties that offer the possibility to have a multi-faced environmental and industrial applications [5] such as CO_2 capture [6], soil amendment [7], water and air treatment [8].

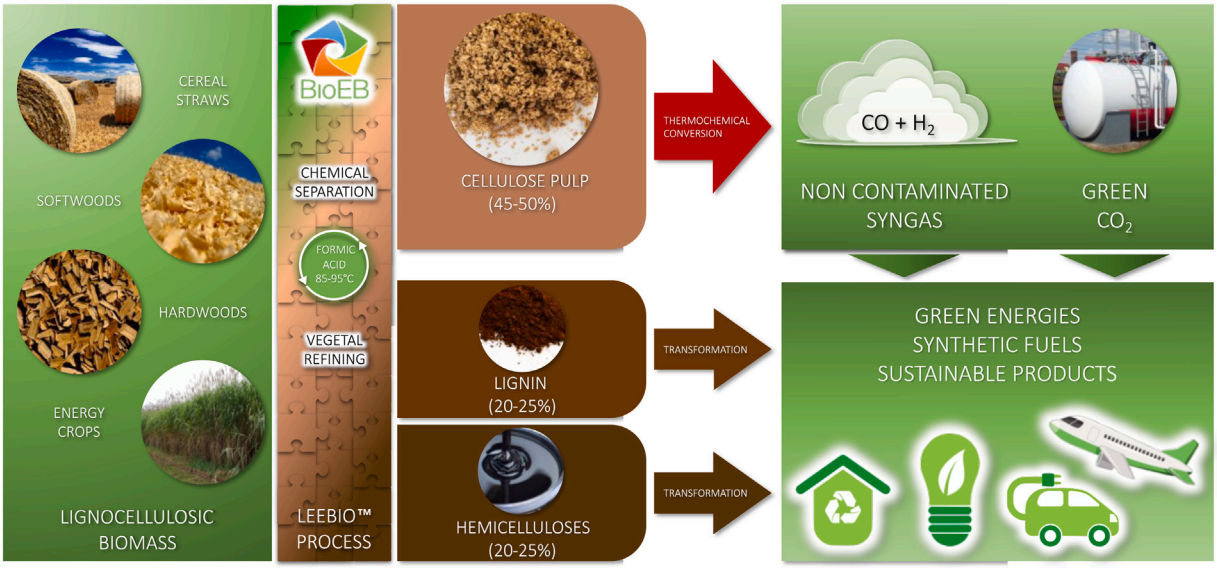

Fig. 1. LEEBIO™ technology – Cellulose pulp, green energies, fuels and products from biomass.

Gasification performance is influenced by a series of factors, notably gasifier type, biomass properties, and operating conditions. Fluidized-bed, entrained flow are the most commonly used gasifiers for clean and efficient production of syngas at large scale [9,10].

The heterogeneity of the feedstock is one of the main issues hampering the ability of gasification reactors to deal with different types of feedstock. Indeed, differences in gasification behavior between various lignocellulosic resources have been highlighted. In literature, there seems to be an agreement on the fact that biochar gasification reactivity is highly influenced by the inorganic matter present in the feedstock [11]. It was indicated that alkali and alkaline earth metals (AAEM), such as Na, K, Mg and Ca have a catalytic impact that enhances biochar gasification [12]. In contrast, other elements, namely Si has the opposite effect and may inhibit the gasification [13]. The effects of catalytic and inhibitor elements have been highlighted using raw biomass and biochar [14–16], acid-washed chars [17–19], and metal-loaded chars [20–23]. The complex effects of AAEM metals on the gasification reactivity, on products distribution and catalytic mechanisms were reviewed [24,25]. Bouraoui et al. [23] studied the effect of K and Si on CO_2 gasification reactivity of a biomass char. When conversion attained 60%, the presence of K and Si became the dominant parameter influencing reactivity. A general trend was obtained between K/Si ratio and reactivity. Few studies have addressed the role of the inorganic matter during biomass constituents gasification, namely cellulose. Gupta et al. [16] compared the gasification behavior of microcrystalline cellulose to alkali lignin. They reported that lignin biochar was more reactive than that of cellulose owing to the high alkali content of lignin. A similar observation was made by Lopez et al. [26]. Most of the current research has focused on the catalytic effect of inorganic elements and its deactivation by the activity of inhibitory elements. However, few studies have addressed the influence of Si content during the gasification of Si-rich bio-resources and the effect of Si removal on biochar gasification. Therefore, the purpose of the present work is to: (1) examine steam gasification of cellulose pulp biochar using TGA; (2) understand the role of the inorganic on biochar reactivity with a focus on Si-content and propose a new approach to predict biochar gasification; (3) investigate the effect of Si elimination on cellulose pulp biochar gasification.

2. Materials and methods

2.1. Raw and extracted materials

Two lignocellulosic biomass residues were selected for this study: wheat straw (WS) and softwood sawdust (SS). Cellulose pulps were extracted from air-dried wheat straw (Cell-WS) and softwood sawdust (Cell-SS).

2.1.1. Cellulose pulp preparation

LeeBio™ Organosolv pretreatment

Biomass pulping was carried out on different scales using *LeeBio™* pretreatment [27]. Cell-SS was obtained from the pulping SS at a pilot scale. At the same time, the Cell-WS was obtained at the lab scale. 40 kg of dried SS (>98%) were mixed with 85 wt. % formic acid, in a 360 L reactor, with a solvent:biomass ratio of 5:1. The mixture was stirred (37 rpm) for 240 min at 85–90 °C at atmospheric pressure. At the end of the cooking, the mixture was cooled to room temperature. First, the media was filtered to separate the raw cellulose pulp from the acid liquor. Second, the pulp was washed with 85 wt.% formic acid, then pressed and filtered. Third, the pulp was washed with warm water, pressed, and filtered until reaching a neutral pH of the filtrate. The pulp was then dried at 60 °C.

WS pulping was conducted in a 1 L reactor following the same protocol described above. 40 g of dried WS (dry matter > 90%) milled to <100 μm were used.

Alkaline treatment

Cell-SS-A is the washed Cell-SS by sodium hydroxide solution. Alka-line treatment was performed to eliminate the remaining silicon in the cellulose pulp. 15 g of dried Cell-SS (>95%) were mixed with 150 mL of water. Approximately, 5 mL of 12 wt. % NaOH solution are then added until pH reaches a value of 11–12 at room temperature. Under stirring, the mixture was heated for 60 min until a stable temperature of 80 °C in the medium. Finally, the cellulose pulp is washed with hot water to reach pH 6–7 to ensure the removal of sodium hydroxide residues.

2.1.2 Characterization

Organic composition

The proximate and ultimate analyses of the samples are shown in Table 1. The content of moisture, ash and volatile matter were

Table 1
Proximate and ultimate composition of the samples.

	WS	Cell-WS	SS	Cell-SS	Cell-SS-A
			Proximate analysis (wt. % db)		
Ash	5.0	4.0	0.3	0.3	0.4
Volatile matter	77.1	86.5	81.5	82.3	84.8
Fixed Carbon[a]	17.9	9.3	18.28	17.5	14.8
			Ultimate analysis (wt. % daf)		
N	0.9	0.1	0.1	0.0	0.0
C	49.5	45.2	47.8	48.5	49.1
H	6.8	6.4	6.2	6.1	6.2
O*	42.8	48.3	45.9	45.4	44.7
			Energy content		
HHV ($MJ\,kg^{-1}$)	19.5	17.4	20.5	19.3	19.7

[a]By difference.

Table 2
Main inorganic elements in the biomass and cellulose pulp samples.

$mg\,kg^{-1}$ (dry basis)	WS	Cell-WS	SS	Cell-SS-P	Cell-SS-A
K	3321	41	340	47	143
Ca	3247	1956	232	273	1943
AAEM	7248	2171	816	353	2713
Fe	138	129	35	89	121
P	621	209	0	0	457
Al	75	135	10	21	34
S	661	49	83	0	0
Si	8789	17259	186	706	268
			K/Si		
	0.4	0.0	1.9	0.0	0.2
			C.I.[a] = (AAEM + Fe)/(Si + Al)		
	0.8	0.1	4.7	0.6	3.9
			% Si		
	52	87	16	61	8

[a]Catalytic Index.

determined according to EN ISO 18134-3, EN ISO 18122 and EN ISO 18123, respectively. Elemental composition was determined by using Themoquest NA 2000 elemental analyzer following EN ISO 16948. The high heating value (HHV) was determined using IKA C 5000 automated bomb calorimeter. The fixed carbon content in the cellulose pulp is lower than the raw biomass due to the higher cellulose content. The ash content in WS is relatively higher than the one in SS sample.

Inorganic composition

In this study, the mineral content of the raw samples was determined using an inductively coupled plasma with atomic emissions spectra (ICP-AES, HORIBA Jobin-Yvon Ultima 2). The concentrations of the major inorganic elements are shown in Table 2. It is essential to underline the difference in the concentration of inorganic species in the raw biomass samples, in particular, the content of silicon. The high amount of the latter in the WS contributes to the plant's stiffness and strength [28].

2.2 TGA gasification experiments

A TG analyzer SETARAM TG-ATD 92 thermal analyzer, coupled with a wet gas generator (Wetsys) was used to perform isothermal gasification experiments. 20 mg of each sample were placed in a cylindrical platinum crucible to experiment as follows (Fig. 2):

1. Under a flow of 1 $L\,min^{-1}$ of nitrogen, the sample was heated to be used to sweep the biochar sample during the heat-up period from room temperature to the gasification temperature (750, 800 and 900 °C). The heat-up was carried out at a constant rate of 10 °C/min.
2. The inert atmosphere was maintained at the desired temperature for 10 min to ensure complete pyrolysis. Thus, both temperature and mass were stabilized.
3. Afterwards, the atmosphere was switched to the gasifying mixture (N_2 + Steam). The total flow rate was set to 4 $L\,h^{-1}$. Different partial steam pressure was used (3.7, 6.2, and 10 kPa) for the gasification of the pyrolysis biochar. The samples were then

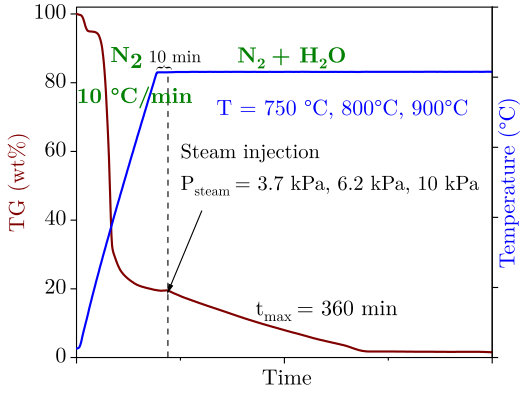

Fig. 2. Experimental procedure and operating conditions (T and P).

kept at the gasification temperature for 360 min. The medium was then cooled down to room temperature.

A blank test was conducted for each test condition to remove the buoyancy effect. The TGA experiments were reproduced to assess repeatability. The calculated standard deviation of the mass loss was below 2%, which is considered to be satisfactory.

2.3 Kinetic analysis approach

As already mentioned above, steam gasification tests were performed isothermally. For each experiment, the approach taken consists of the following steps:

- The degree of conversion α was calculated following:

$$\alpha = \frac{m_0 - m_{(t)}}{m_0 - m_{ash}} \quad (1)$$

Where m_0 is the biochar mass at the end of the pyrolysis stage, m_{ash} is the sample ash content determined with TGA experiments, and $m(t)$ is the mass at a given time t of the analysis. $m(t)$ values were collected every 1.8 s.

- The biochar gasification rate is defined as the variation of the conversion degree α vs time:

$$r = \frac{d\alpha}{dt} \quad (2)$$

- The apparent reactivity $R(\alpha)$ in %.min^{-} can be obtained from the conversion degree and the reaction rate following:

$R(\alpha) = \frac{1}{(3)}\frac{d\alpha}{1-\alpha\, dt}$

The average reactivity over a defined conversion range can be then expressed by the average of the apparent reactivities at each α.

- Typically, the overall biochar gasification rate can be expressed by:

$r = \frac{d\alpha}{dt} = A\, exp(-Ea/RT) \times h(P_{H_2O}) \times f(\alpha)$ (4)

where A is the pre-exponential factor min^{-1}, Ea is the apparent activation energy (kJ mol^{-1}), and R is the universal gas constant (8.314 J mol^{-1} K^{-1}), and T is the gasification temperature. h(P_{H_2O}) describes the dependence on the partial pressure of the gasifying agent. It is assumed to follow a power law:

$g(P_{H_2O}) = P^{m}_{H_2O}$

- An isoconversional model-free approach was used to determine the activation energy and the pre-exponential factor. In this approach, the reaction rate is assumed to be only function of time at a constant conversion degree. Thus, the apparent energy Ea can be calculated without knowing the reaction mechanism. The calculation of A depends on the previous knowledge of the reaction model
- The generalized master-plots method was used for determin-ing the reaction mechanism ($f(\alpha)$), as described in a previous study [29]. The reduced-generalized reaction rate can be deter-mined from the experimental kinetic data:

$\lambda(\alpha) \equiv \frac{f(\alpha)}{exp(Ea/RT_{\alpha=0.5})} = \frac{d\alpha/dt\, exp(Ea/RT)}{f(\alpha)_{\alpha=0.5}\,(d\alpha/dt)_{\alpha=0.5}}$ (5)

Fig. 3 shows the theoretical master plots functions of the most commonly used mechanisms. For isothermal programs, the previous knowledge of the activation energy is not required. Thus, the exponential terms in Eq. (5) can be canceled out. Hence, the experimental master plots can be established directly from an dα/dt curve [30]. The most suitable reaction mechanism is the one theoretical plot that gives the best match to the experimental plots [31].

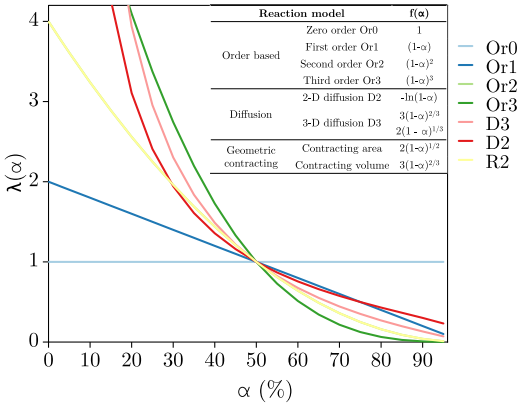

Fig. 3. Most common reaction mechanisms and their corresponding generalized master plots.

3 Results and discussion

3.1 Effect of acid pulping and the alkaline treatment on the cellulose ash composition

Compared with raw biomass, *LeeBio*™ cellulose pulp is sulfur and nitrogen-free which are the precursors of pollutants in the syngas [4]. As it can be seen from Table 2, and TEM-EDX images (supporting information), the ash composition of the extracted cellulose pulp is different from the raw biomass. Significant fractions of AAEM species were eliminated during formic acid pulping, whereas Si was the dominant element in the extracted cellulose ash. Regarding biomass extraction, inorganic salts containing AAEM are dissolved under acidic conditions. Whereas Si compounds are retained in the pulp after the acid treatment inside the cellulose pulp fibers [32,33], precisely in the epidermic cells [34]. It is important to point out that Si derivatives in the cellulose pulp are mostly silica and calcium silicate [35].

The efficiency of the alkaline washing on the elimination of Si derivatives can be illustrated by a decrease of 65% between Cell-SS and Cell-SS-A. However, the rise of AAEM content that was not present in the acid pulp may be due to the inorganic species in some impurities in the chemical itself. Moreover, as after the alkaline wash parts of the biomass elements are removed from the sample, the relative amount of these impurities increases.

3.2 Influence of the inorganic content on the cellulose pulp biochar reactivity

The conversion curves *vs* time of different biochar samples at different temperatures are shown in Fig. 4. As expected, the gasification temperature has a significant impact on biochar reactivity. The temperature increase led to a considerable increase in reactivity, which reduces the reaction time. Table 3 provides an overview of reaction time, maximum conversion degree and the reactivity of all analyzed materials. A complete biochar conversion was obtained at 900 °C, while the full conversion at 800 °C and 750 °C after 300 min was below 60% for Cell-SS and Cell-WS biochars. These findings are in agreement with previous studies on the reaction temperature effect for both steam and CO_2 gasification of biomass biochars [36–38].

From Fig. 4, it is clear that the gasification behavior of cellulose pulp biochars is different from their raw biomass biochars. Table 3 reveals the difference in reactivities between cellulose pulp and raw biomass biochars at different temperatures. The pulp biochar displayed lower reactivity than the raw biomass biochars. A factor of 3 between the reactivities of raw biomass and cellulose pulp biochars at 800 °C was found. At 900 °C, the reaction time of Cell-SS and Cell-WS biochars is

Table 3
Char steam gasification reactivity at 30% conversion $R_{30\%}$, maximum conversion level after 360 min of reaction α_{max}, and its corresponding reaction time $t_{\alpha_{max}}$; partial steam pressure 6.2 kPa.

		WS	Cell-WS-L	SS	Cell-SS-P
750 °C	$R_{30\%}$ (%.min^{-})	0.55	0.07	0.30	0.09
	α_{max} (%)	79.3	44.2	95.0	35.4
			$t_{\alpha_{max}}$ =360 min		
800 °C	$R_{30\%}$ (%.min^{-})	1.32	0.52	1.21	0.44
	α_{max} (%)	94.9	78.2	100	82.5
	$t_{\alpha_{max}}$ (min)	360	360	139.2	360
900 °C	$R_{30\%}$ (%.min^{-})	6.2	2.69	4.33	2.98
			α_{max} = 100%		
	$t_{\alpha_{max}}$ (min)	53.2	178.8	34.5	117.3

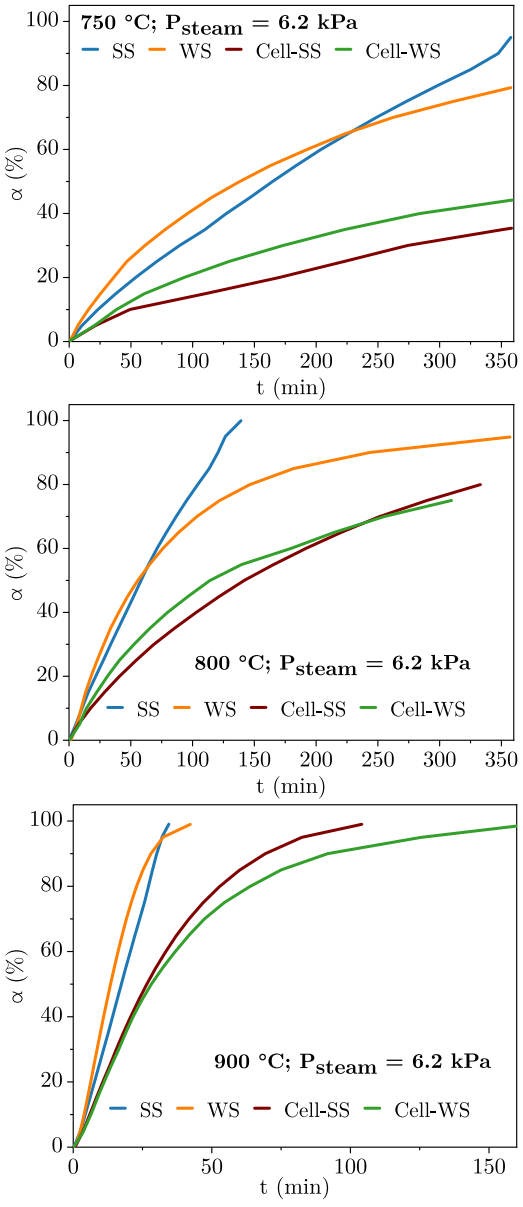

Fig. 4. Conversion degree α *vs* time of different biochar samples at different temperatures with a partial steam pressure of 6.2 kPa.

117 min and 178 min, respectively, to obtain a 100% biochar conversion. The reaction time of raw biomass biochars is 34 min and 42.2 min for (6) SS and WS, respectively. This steep difference in the reaction time between the raw biomass and the cellulose pulp biochars could generate a significant difference at a large scale, particularly for the residence time in the gasification reactor.

Such difference cannot be explained by the difference in macromolecular composition in terms of lignin, cellulose and hemicelluloses [16,24]. Gasification behavior seemed to be linked to the inherent inorganic elements in the lignocellulosic material, such as AAEM, Si, Al, and P. AAEM are known to be catalysts for the steam gasification reactions. The dominant catalytic effect is exhibited by K-species [19, 21,22]. In contrast, Si, Al, and P are reported to have inhibiting effect on the gasification. Specifically, inherent Si compounds such as SiO2 tend to inhibit K-catalysis [39]. Therefore, the raw biomass biochars, which contain AAEM species, had higher reactivities than pulp biochars. Since most of AAEM salts had been eliminated under acidic conditions during pulping, their concentration in the cellulose pulp was drastically reduced.

Different inorganic ratios have been used in the literature to highlight the catalytic effect of K and other AAEM species and the inhibitor effect of Si, as seen in Table 4. According to Dupont et al. [14], the reaction rate was constant for biomass with K/(Si+P) > 1, in contrast the rate decreased along conversion for biomass with ratio K/(Si+P) < 1. Romero Millan et al. [29] studied steam gasification on tropical biomass. A linear relationship was found between the biomass reactivity and the inorganic ratio K/(Si+P) of samples, in the analyzed temperature range. Alkali or catalytic index (C.I.) has also been used to correlate the reactivity to the inorganic content. Other studies found a correlation between the reactivity and the content of K, Na, and Ca. However, the use of one of these inorganic ratios is limited in our case since there is a steep difference in K content between raw biomass and the cellulose pulp, as shown in Table 2. As mentioned above, Si is present in the ash from different materials and is the main element in pulp ash. Therefore, the %Si index calculated as follows was used in the analysis of the gasification kinetics:

$$\%\ \mathrm{Si} = \frac{\mathrm{Si\ (mg\ kg^{-1})}}{Total\ major\ inorganic\ elements\ (\mathrm{mg\ kg^{-1}})}\ (wt.\%) \qquad (6)$$

%Si for SS sample was 16%, while that for WS, Cell-WS and Cell-SS samples were higher than 50%. In order to verify the effect of Si, in particular on cellulose pulp gasification, the variation of reaction rate over the conversion is presented in Fig. 5. The studied biochar samples can be classified into two groups:

- This first group is represented by SS sample: the conversion increases as a straight line. The reaction rate is constant with increasing carbon conversion until about 80%. Since its low content in SS, no inhibitory effect of Si on the gasification rate was identified. A significant increase in reaction rate was observed at higher conversion. This finding is in line with other studies using woody biomass with similar inorganic content [23,40]. This trend was explained by the fact that AAEM are more concentrated at higher conversion which could enhance the catalytic effect [24].

Table 4
Char gasification studies taking into account inorganic elements (LB: Lignocellulosic Biomass; PC: Petroleum Coke).

Feedstock	Agent T (°C)	Main findings
		K/(Si+P)
LB MA	H_2O 800	K/(Si+P)> 1, constant reaction rate (Or0). K/(Si+P)<1, decreasing reaction rate (Or1). [14]
LB Algae	H_2O 800	K/(Si+P)> 1, constant reaction rate; K/(Si+P)<1, decreasing reaction rate; Si and P tend to encapsulate P species and limit its catalytic activity. [40]
LB	H_2O 750–950	Reactivity increases while reaction order decreased with increasing K/(Si+P); K/(Si+P)>1, Or0; K/(Si+P)<1 reaction order > 1 and can be a function of K/(Si+P). [29]
		K/Si
LB	H_2O 750–900	A factor of 3.5 is found between the average reaction rate of various wood biochars. Reaction rate is correlated to K/Si. [41]
LB	H_2O 650–800	Reactivity is correlated with K/Si for five of the six biochars. Ca content in the sixth sample is high. [42]
Char	CO_2 800	X > 60%, reactivity was influenced by the presence of K and Si. Reactivity was correlated to K/Si at X > 50%. [23]
		Catalytic Index (alkali index) C.I. = (K+Ca+Na+Mg+Fe)/(Si+Al)
LB	CO_2 800	Reactivity increases with increasing C.I. Average reaction rate is correlated to C.I. at higher conversion. [43]
LB	CO_2 800	Reactivity increases with increasing C.I. Modified random pore model can describe biochar gasification. [16]
LB Coal	CO_2 800	K has the major catalytic contribution. At T > 800 °C, K catalytic effect is reduced as it forms salts with Si and Al.[44]
LB	H_2O 900	Good correlation of biochar reactivity with (C.I.). Random pore model can describe kinetics using an additional term correlated to [Ca]. [26]
LB- PC Coal	CO_2 850–1000	No relationship between the reactivity and alkali index of chars. [45]
		(K+Na+Mg)/(Si+Al+P+Ca)
LB	H_2O 750–1000	This index is the most suitable to explain the reactivity among different index used. [15]
		(Na+Ca+K)
LB	H_2O 900	3 groups are identified. Group I: [Na]+[K] > [Ca]; highest reactivity; Group II: [Ca] > [Na]+[K]; Group III: has the lowest reactivity dut to the high silica content; A random pore model related to K content is used. [20]
LB	H_2O, CO_2 800–1300	Reactivity increases with increasing ([Na]+[K]). [46]

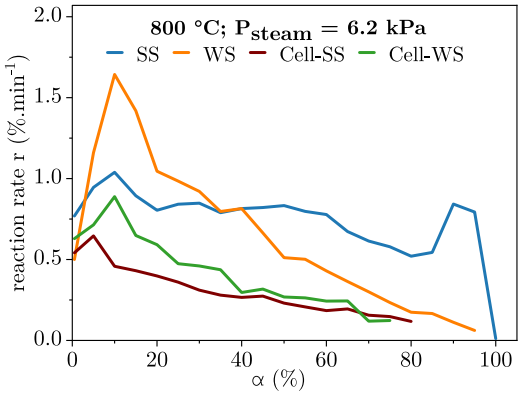

Fig. 5. Experimental reaction rate as a function of conversion, at 800 °C with a partial steam pressure 6.2 kPa.

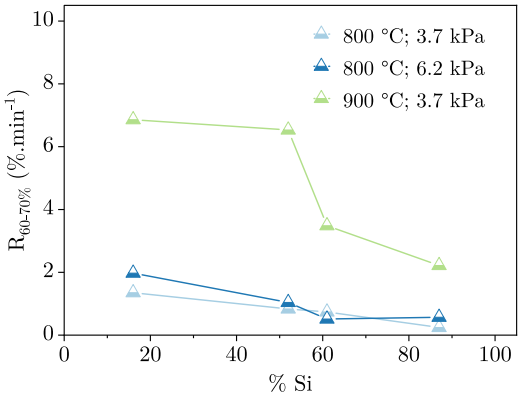

Fig. 6. Average reactivity at selected conversion range as a function of %Si (curves are just shown to highlight the tendencies).

- The second group includes WS, Cell-WS and Cell-SS samples: a maximum reaction rate at earlier conversion levels, then the conversion increases with a decreasing reaction rate. The decrease of reaction rate with conversion confirms the inhibitory effect of Si on biochar gasification. It should be underlined that the overall shape of the gasification rate profile was similar. After reaching the maximum at a lower conversion level, the reaction rate decreases with increasing conversion. As the carbon is consumed, Si concentration increases, leading to a steep drop in the reaction rate. According to literature, the decreasing rate is related to the tendency of silica to encapsulate AAEM species to form inactive silicate complex oxides, which are stable and non-catalytic compounds [20,40]. However, these complexes are in much smaller amounts in the case of cellulose pulp biochar due to the reduced amount of AAEM. Two other different phenomena explaining the inhibitory effect were mentioned in the literature. Gupta et al. [16] reported that the inhibition of biochar gasification can be caused by the bonding of silica with carbon. Lu et al. [47] reported that a high dispersion of Si on biochar can prevent the transformation of oxygen and slow the gasification down.

In order to validate our prediction, all the samples were combined by correlating %Si with the biochar reactivity. The average reactivity as a function of %Si is shown in Fig. 6. As can be seen, a general trend for biochar gasification reactivity as a function of %Si can be established. The reactivity decreased with increasing %Si ratio. This confirms the inhibitory effect of Si and reveals that pulp biochar reactivity is governed by %Si.

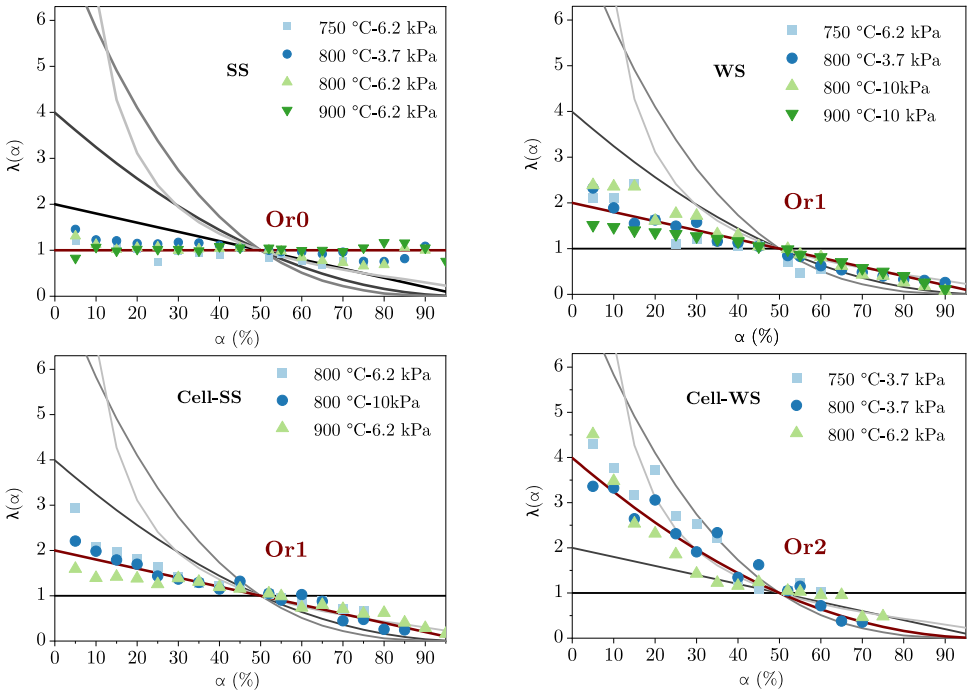

Fig. 7. Comparison between theoretical master-plots and experimental plots against α for different samples.

Besides the effect of the inorganic composition, the morphological structure of biochar is another parameter that can also influence biochar reactivity. This parameter has been less covered in the literature than the inherent inorganic composition. The morphological structure is particularly influenced by the release of the volatile species during the pyrolysis which is controlled by the heating rate [48]. For slow heating rate as the one used in this study, no major modification occurs in the particle morphology [49], biochars from low heating rate pyrolysis keep their raw porosity. As shown in Fig. 5, the reactivity of WS biochar is greater than that of SS. The same behavior was also observed when comparing Cell-WS and Cell-SS, considering that acid pulping does not have major effect on the morphological structure. This trend is reversed at subsequent stages of conversion and assessed with the inorganic content. Therefore, this result indicates that the biochar structure might have a slight effect on biochar reactivity at earlier stage of conversion. With increasing conversion, the concentration of inorganic elements increases, hence their catalytic or inhibitor effect is stronger, becoming the main parameter governing biochar gasification. In this regard, Di Blasi [50] also reported that morphological structure seemed to be less affecting than the inorganic content.

3.3 Gasification kinetics analysis

Prior to calculating Ea and A, the dependence on the partial pressure of the gasifying agent and the reaction mechanism were elucidated. The reaction order with respect to steam partial pressure is represented by the slope of the log–log plot of dα/dt *vs* partial steam pressure at fixed conversion. It was calculated at three different pressure. No signif-icant variation with conversion was observed. The obtained value was about 0.66, which ties well with the values reported in the literature (0.4–1) [50].

$f(\alpha)$ is a function that is associated with a physical model that describes the kinetics of the solid-state reaction. Generally, *n*th-order models particularly the volumetric reaction model, shrinking core model, and random pore model are the most commonly used applied kinetics models to describe heterogeneous gas–solid reactions [51]. The above-mentioned models can be modified to take into account the effect of inorganic content. For instance, several kinetic models have been proposed taking into account inorganic content particularly K and Ca with and without considering Si. Volumetric models using K/(Si+P) ratio have been used to predict steam gasification behavior of different biomass biochars [14,29]. A random pore model with additional factor correlated to K content was used to describe steam gasification of biomass biochar [20,52]. Grain model with additional factor function of (K/Si) [41], and Ca content [26,52] was also used tp describe steam gasification kinetics.

To determine the suitable kinetic model describing biochar gasification, generalized master plots were used. Theoretical master plots $f(\alpha)/f(\alpha)_{\alpha=0.5}$ for various kinetic models and experimental curves $\frac{d\alpha/dt}{(d\alpha/dt)_{\alpha=0.5}}$ against α are presented in Fig. 7. As can be noted, no variation was observed in the kinetic model for all studied samples with temperatures and partial steam pressure. This confirms the independence of the decomposition mechanism from the operating conditions [53].

Regarding the kinetic model, it can be seen that *n*th-order based mechanisms could be noticed in the steam gasification of biomass and cellulose pulp biochars. The generalized master-plots curves show that the zero-order model is the most suitable mechanism model $f(\alpha)$ for SS biochar (group 1) with low Si content. The gasification rate is constant up to a conversion level of 80%.

On the other hand, it is apparent that the reaction mechanisms shift up to a higher reaction-order. The first-order mechanism gives the best match with the experimental data for WS. A first-order mechanism is also responsible for the Cell-SS gasification. This similar reaction order identified for the two samples can be explained by the similarity of %Si. The reaction mechanism of Cell-WS biochar gasification is close to second-order (Or2). This observation confirms the inhibitory effect of Si, where a decrease in the gasification rate is observed with increasing %Si.

From the data, a linear relationship between the reaction order n and %Si can be established, as shown in Fig. 8. The reaction order increase with the increase of %Si. Consequently, the gasification behavior of the cellulose pulp biochar can be described using their silica content. The activation energy *Ea* was calculated from the slope of the plot ln(t) *vs* T^{-1}, for constant values of α. A mean value of 149.7 kJ mol^{-1} was calculated for all biochar samples. These results

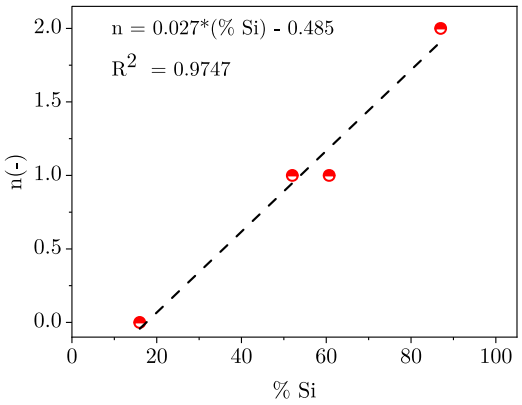

Fig. 8. Reaction order n as a function of %Si.

Table 5
Kinetic parameters of different biochar samples.

	A (min kPa$^{-0.66}$)	Ea (kJ mol^{-1})
SS	4.0×10^{6}	149.7±2.5
Cell-SS-P	2.4×10^{4}	
WS	5.8×10^{4}	
Cell-WS-L	4.8×10^{6}	

are in accordance with results reported in the literature [29,54,55]. Afterwards, the pre-exponential factor was determined using Eq. (4). The obtained values are listed in Table 5. No apparent relationship was found between the kinetic parameters, A and Ea and the inorganic content. For biomass biochar, the value of A was higher for sample samples with low Si content. For cellulose biochars, the order of magnitude of this parameter was similar for the Cell-SS and Cell-WS, which have a low K concentration. Since the limited number of analyzed pulp biochar samples and their low K content, the kinetic parameter cannot be correlated to the inorganic content. The overall equation describing the gasification kinetic behavior rate was then expressed as follows:

$$\frac{d\alpha}{dt} = A \times exp(\frac{-149700}{RT}) \times P_{H_2O}^{0.66} \times (1-\alpha)^{n}$$
$$n = 0.027 \times (\%Si) + 0.48 \quad (7)$$
$$\%Si = [0\text{–}100\%];\ P_{H_2O} = [3.7\text{–}10\ kPa]$$

3.4 Kinetic model accuracy

To assess accuracy of the model, predicted reaction rate was compared with the experimental results. The deviation was quantified using Nonlinear Least Squares:

$$Dev\,(\%) = 100\,\frac{\sqrt{\sum_{j=1}^{n}[\alpha_{exp,j} - \alpha_{calc,j}]^2}}{\sqrt{N}\,\alpha_{exp,max}} \quad (8)$$

where N is the number of experimental points employed; α_{exp} and α_{calc} are respectively the experimental and predicted model biochar conversion rates. The deviation (min–max) for SS, WS, Cell-SS and Cell-WS was respectively 1.6–5.2, 2.2–5.0, 1.9–5.0 and 2.4–9.1% indicating that the model agrees well with the experimental results. Graphical comparisons between the breakthrough data and the data obtained from the model in Eq. (7) are given in Fig. 9. As illustrated, the modeled data off all analyzed samples fitted sufficiently well with the experimental conversion profile vs time. This offers the potential of using Si content to describe the gasification behavior of a wide range of materials including cellulose pulp biochar. Most importantly, the gasification behavior of cellulose pulp biochars can be predicted despite the low content of AAEM species, particularly potassium. It should be emphasized that the linear relationship used to predict the reaction order from %Si was used to reproduce the results of other studies [14,29,40] in which they used inorganic ratios such K/Si and K/(Si+P). A very good agreement was found between the results for determining the reaction order except in the case of biomass having high phosphorous content (supporting information).

3.5 Effect of silica elimination on biochar reactivity

The above results fully depict the significant difference in steam gasification behavior of the raw biomass and the cellulose pulp biochars. The pulp biochar gasification is governed by Si content. The severe inhibitory effect of Si on the pulp biochar gasification leads to lower reactivities which subsequently result in a more extensive reaction time. The elimination of Si is expected to increase the reactivity of pulp biochar. Fig. 10 shows the comparison between the conversion profiles of raw biomass, cellulose pulp and the alkaline-washed pulp. Cell-SS-A showed higher reaction rate than Cell-SS, which Si is its main inorganic element. Si species, mainly found in the epidermic cells, are considerably removed through the alkaline treatment. Hence, biochar gasification reactivity increases. At low conversion, Cell-SS-A and SS biochars have almost similar reactivities. For the alkaline-washed pulp biochar, the trend of variation of reaction rate over the whole conversion range did not show any increase. The behavior of alkaline-washed pulp can be compared to other studies in which the effect of acid washed was elucidated in the absence of Si. Indeed, different studies have reported lower reactivities for acid washed biochar in absence of Si. Yip et al. [17] found that the reactivity of acid-treated biochar had much lower reactivity than raw biochar, and its reactivity remained constant throughout the whole conversion range. Lower reactivities for raw biochars were reported for acid-washed biochars [18,19,56].

In Table 6 the reactivity and reaction time at operating conditions are highlighted. The results provide important insights into the beneficial impact of Si removal on cellulose pulp biochar gasification. For instance, it can be noticed that the reactivity increased 2.5 and 1.3 times at 800 and 900 °C with a partial steam pressure of 3.7 kPa, respectively. At 800 °C, the reaction time to achieve 70% of biochar conversion was reduced from 357.0 and 201.0 min to 139.2 and 87.0 min with a partial steam pressure of 3.7 and 10 kPa, respectively. Hence, the required reaction time to achieve 70% of conversion was reduced by 60%. The same trend was observed at 900 °C where the reaction time was reduced by 22 and 32% with a partial steam pressure of 3.7 and 10 kPa, respectively. The reduction of Si content leads to an increase in biochar reactivity and a decrease in the reaction time. Cell-SS-A biochar had a slightly lower reactivity than the raw biomass biochar.

4 Conclusion

In the present study, sulfur and nitrogen-free cellulose pulp, obtained using an innovative technology, was used for steam gasification. The tests were performed using isothermal conditions. The results were compared to the raw biomass. The significant difference in AAEM and Si contents could lead to a major difference in gasification behavior. Slower gasification than the raw biomass biochar was observed. The cellulose biochar was 3 times lower than from biomass. The gasification behavior of extracted cellulose biochar was predominantly governed by Si concentration cellulose. A less significant impact attributed to the morphological structure was also observed.

A new modeling approach based on Si concentration was proposed to predict the steam gasification kinetics of lignocellulosic biomass and cellulose chars. The TGA data and the derived model showed a satisfactory agreement with a deviation below 10%.

The elimination of Si species by NaOH based alkaline washing enabled the enhancement of cellulose biochar gasification toward H_2-rich syngas production. The biochar reactivity increased 2.5 and 1.3 times

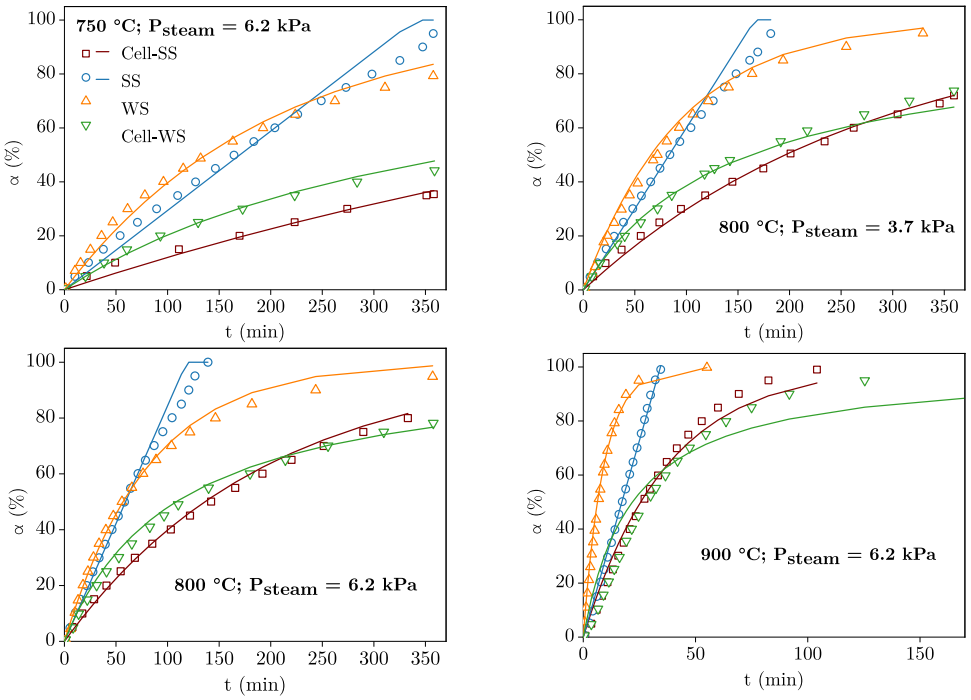

Fig. 9. Comparison between experimental conversion data and the modeled conversion curves of all studied samples under different operating conditions. (scatter: experimental data; line: model-predicted results).

Table 6
Gasification reactivity and the required time to achieve 70% conversion at different operating conditions.

α = 70%	800 °C; 3.7 kPa		800 °C; 10 kPa		900 °C; 3.7 kPa		900 °C; 6.2 kPa	
	R	t	R	t	R	t	R	t
SS	1.51	126.0	2.84	64.8	8.06	28.8	9.74	24.0
Cell-SS-P	0.34	357.0	0.45	201.0	3.71	46.2	3.58	41.7
Cell-SS-A	0.87	139.2	1.35	87.0	4.87	36.0	6.14	28.5

R unit is %.min^{-}; t unit is min.

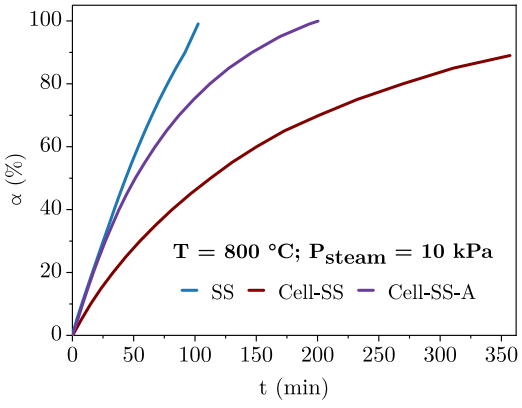

Fig. 10. Conversion degree α *vs* time for of SS, Cell-SS, and Cell-SS-A biochars at 800 °C with a partial steam pressure of 10 kPa.

at 800 and 900 °C, respectively. Hence, the results of the present investigation confirmed that Si content is a principal influencing parameter on biochar kinetics.

With the complexity of gasification process, other factors which have not been taken in consideration in the model. For instance, gasification tests needs to be extended to other biochars with different morphological properties such as surface area, pore volume and surface texture. The gasification in CO_2 atmosphere and CO_2/H_2O mixture would also be worth to be addressed in a follow-up research.

CRediT authorship contribution statement

Majd Elsaddik: Conceptualization, Investigation, Methodology, Writing – original draft. **Ange Nzihou:** Conceptualization, Supervision, Funding acquisition. **Michel Delmas:** Resources, Conceptualization, Funding acquisition. **Guo-Hua Delmas:** Resources, Conceptualization, Funding acquisition.

Declaration of competing interest

The authors declare the following financial interests/personal relationships which may be considered as potential competing interests: Ange Nzihou reports financial support was provided by Occitanie Region. Ange Nzihou reports financial support was provided by BioEB Auzeneville-Tolosane France. Majd Elsaddik has patent #FR2206388 pending to BioEB, Auzeneville-Tolosane, France.

Data availability

Data will be made available on request.

Acknowledgments

This research has been funded by La Région Occitanie (ARRÊTÉ N° 19008756/ALDOCT-00802) and the group BioEB.

References

[1] Nalley S, LaRose A. International Energy Outlook 2021. 2021, p. 21, URL https://www.eia.gov/outlooks/ieo/.

[2] International Energy Agency. World Energy Outlook 2021. 2021, p. 386, URL https://www.iea.org/reports/world-energy-outlook-2021.

[3] European Commission. State of play on the sustainability of solid and gaseous biomass used for electricity, heating and cooling in the EU. 2014, URL https: //ec.europa.eu/energy/topics/renewable-energy/biomass_en.

[4] Delmas G-H, Banoub JH, Delmas M. Lignocellulosic biomass refining: A review promoting a method to produce sustainable hydrogen, fuels, and products. Waste Biomass Valoris 2021. http://dx.doi.org/10.1007/s12649-021-01624-6, URL https://link.springer.com/10.1007/s12649-021-01624-6.

[5] Singh E, Mishra R, Kumar A, Shukla SK, Lo S-L, Kumar S. Circular economy-based environmental management using biochar: Driving towards sustainability. Process Saf Environ Prot 2022;163:585–600.

[6] Kumar A, Singh E, Mishra R, Lo S-L, Kumar S. A green approach towards sorption of CO2 on waste derived biochar. Environ Res 2022;214:113954.

[7] Karim AA, Kumar M, Singh E, Kumar A, Kumar S, Ray A, et al. Enrichment of primary macronutrients in biochar for sustainable agriculture: A review. Crit Rev Environ Sci Technol 2022;52(9):1449–90.

[8] Kumar A, Singh E, Mishra R, Kumar S. Biochar as environmental armour and its diverse role towards protecting soil, water and air. Sci Total Environ 2022;806:150444.

[9] Krzywanski J, Fan H, Feng Y, Shaikh AR, Fang M, Wang Q. Genetic algorithms and neural networks in optimization of sorbent enhanced H2 production in FB and CFB gasifiers. Energy Convers Manage 2018;171:1651–61.

[10] Gao M, Xiao Y, Chen Z, Ding L, Gao Y, Dai Z, et al. Comparison of physicochemical properties and gasification reactivity of soot from entrained flow gasification processes. Chem Eng J 2022;450:136660.

[11] Zhang Y, Wan L, Guan J, Xiong Q, Zhang S, Jin X. A review on biomass gasification: effect of main parameters on char generation and reaction. Energy Fuels 2020;34(11):13438–55. http://dx.doi.org/10.1021/acs.energyfuels.0c02900, URL https://pubs.acs.org/doi/10.1021/acs.energyfuels.0c02900.

[12] Nzihou A, Stanmore B. The fate of heavy metals during combustion and gasification of contaminated biomass—A brief review. J Hazard Mater 2013;256–257:56–66. http://dx.doi.org/10.1016/j.jhazmat.2013.02.050, URL https://linkinghub.elsevier.com/retrieve/pii/S0304389413001660.

[13] Strandberg A, Holmgren P, Wagner DR, Molinder R, Wiinikka H, Umeki K, et al. Effects of pyrolysis conditions and ash formation on gasification rates of biomass char. Energy Fuels 2017;31(6):6507–14. http://dx.doi.org/10.1021/acs.energyfuels.7b00688, URL https://pubs.acs.org/doi/10.1021/acs.energyfuels.7b00688.

[14] Dupont C, Jacob S, Marrakchy KO, Hognon C, Grateau M, Labalette F, et al. How inorganic elements of biomass influence char steam gasification kinetics. Energy 2016;109:430–5. http://dx.doi.org/10.1016/j.energy.2016.04.094, URL https://linkinghub.elsevier.com/retrieve/pii/S0360544216305072.

[15] González-Vázquez M, García R, Gil M, Pevida C, Rubiera F. Unconventional biomass fuels for steam gasification: Kinetic analysis and effect of ash composition on reactivity. Energy 2018;155:426–37. http://dx.doi.org/10.1016/j.energy.2018.04.188, URL https://linkinghub.elsevier.com/retrieve/pii/S0360544218308132.

[16] Gupta A, Thengane SK, Mahajani S. CO2 gasification of char from lignocellulosic garden waste: Experimental and kinetic study. Bioresour Technol 2018;263:180–91. http://dx.doi.org/10.1016/j.biortech.2018.04.097, URL https://linkinghub.elsevier.com/retrieve/pii/S0960852418306205.

[17] Yip K, Tian F, Hayashi J-i, Wu H. Effect of alkali and alkaline earth metallic species on biochar reactivity and syngas compositions during steam gasification. Energy Fuels 2010;9.

[18] Mitsuoka K, Hayashi S, Amano H, Kayahara K, Sasaoaka E, Uddin MA. Gasification of woody biomass char with CO2: The catalytic effects of K and Ca species on char gasification reactivity. Fuel Process Technol 2011;92(1):26–31. http://dx.doi.org/10.1016/j.fuproc.2010.08.015, URL https://linkinghub.elsevier.com/retrieve/pii/S0378382010002791.

[19] Kajita M, Kimura T, Norinaga K, Li C-Z, Hayashi J-i. Catalytic and noncatalytic mechanisms in steam gasification of char from the pyrolysis of biomass †. Energy Fuels 2010;24(1):108–16. http://dx.doi.org/10.1021/ef900513a, URL https://pubs.acs.org/doi/10.1021/ef900513a.

[20] Zhang Y, Ashizawa M, Kajitani S, Miura K. Proposal of a semi-empirical kinetic model to reconcile with gasification reactivity profiles of biomass chars. 2008, p. 7.

[21] Huang Y, Yin X, Wu C, Wang C, Xie J, Zhou Z, et al. Effects of metal catalysts on CO2 gasification reactivity of biomass char. Biotech Adv 2009;5.

[22] Pflieger C. Catalytic influence of mineral compounds on the reactivity of cellulose-derived char in O2-, CO2-, and H2O-containing atmospheres. 2021, p. 11.

[23] Bouraoui Z, Dupont C, Jeguirim M, Limousy L, Gadiou R. CO2 gasification of woody biomass chars: The influence of K and Si on char reactivity. C R Chimie 2016;19(4):457–65. http://dx.doi.org/10.1016/j.crci.2015.08.012, URL https://linkinghub.elsevier.com/retrieve/pii/S1631074816000138.

[24] Dahou T, Defoort F, Khiari B, Labaki M, Dupont C, Jeguirim M. Role of inorganics on the biomass char gasification reactivity: A review involving reaction mechanisms and kinetics models. Renew Sustain Energy Rev 2021;135:110136. http: //dx.doi.org/10.1016/j.rser.2020.110136, URL https://linkinghub.elsevier.com/retrieve/pii/S1364032120304275.

[25] Yu J, Guo Q, Gong Y, Ding L, Wang J, Yu G. A review of the effects of alkali and alkaline earth metal species on biomass gasification. Fuel Process Technol 2021;214:106723. http://dx.doi.org/10.1016/j.fuproc.2021.106723, URL https: //linkinghub.elsevier.com/retrieve/pii/S0378382021000023.

[26] López-González D, Fernandez-Lopez M, Valverde J, Sanchez-Silva L. Gasification of lignocellulosic biomass char obtained from pyrolysis: Kinetic and evolved gas analyses. Energy 2014;71:456–67. http://dx.doi.org/10.1016/j.energy.2014.04.105, URL https://linkinghub.elsevier.com/retrieve/pii/S0360544214005362.

[27] Delmas M. A low energy production process for producing paper pulp from lignocellulosic biomass. 2019, URL https://patentscope.wipo.int/search/en/detail.jsf?docId=WO2019158247.

[28] Vassilev SV, Baxter D, Andersen LK, Vassileva CG. An overview of the chemical composition of biomass. Fuel 2010;89(5):913–33. http://dx.doi.org/10.1016/j.fuel.2009.10.022, URL https://linkinghub.elsevier.com/retrieve/pii/S0016236109004967.

[29] Romero Millán LM, Sierra Vargas FE, Nzihou A. Steam gasification behavior of tropical agrowaste: A new modeling approach based on the inorganic composition. Fuel 2019;235:45–53. http://dx.doi.org/10.1016/j.fuel.2018.07.053, URL https://linkinghub.elsevier.com/retrieve/pii/S0016236118312523.

[30] Sánchez-Jiménez PE, Pérez-Maqueda LA, Perejón A, Criado JM. Generalized master plots as a straightforward approach for determining the kinetic model: The case of cellulose pyrolysis. Thermochimica Acta 2013;552:54–9. http://dx.doi.org/10.1016/j.tca.2012.11.003, URL https://linkinghub.elsevier.com/retrieve/pii/S0040603112005278.

[31] Pham Minh D, Accart P, Boachon C, Calvet R, Chesnaud A, Del Confetto S, et al. Generic and advanced characterization techniques. In: Nzihou A, editor. Handbook on characterization of biomass, biowaste and related by-products. Springer International Publishing; 2020, p. 31–497. http://dx.doi.org/10.1007/978-3-030-35020-8_2, ISBN: 978-3-030-35019-2.

[32] Pan X, Sano Y. Fractionation of wheat straw by atmospheric acetic acid process. Bioresour Technol 2005;96(11):1256–63. http://dx.doi.org/10.1016/j.biortech.2004.10.018, URL https://linkinghub.elsevier.com/retrieve/pii/S0960852404003773.

[33] Sinha ASK. Formic acid pulping process of rice straw for manufacturing of cellulosic fibers with silica. TAPPI J 2021;20(8):489–96. http://dx.doi.org/10.32964/TJ20.8.489, URL https://imisrise.tappi.org/TAPPI/Products/21/AUG/21AUG489.aspx.

[34] Sun L, Gong K. Silicon-based materials from rice husks and their applications. Ind Eng Chem Res 2001;40(25):5861–77. http://dx.doi.org/10.1021/ie010284b, URL https://pubs.acs.org/doi/10.1021/ie010284b.

[35] Lam HQ, Le Bigot Y, Ghislain D, Thao VH, Delmas M. Location and composition of silicon derivatives in rice straw pulp obtained by organic acid pulping. 2005, p. 4, 58 (3).

[36] Link S, Arvelakis S, Hupa M, Yrjas P, Külaots I, Paist A. Reactivity of the biomass chars originating from Reed, Douglas Fir, and Pine. Energy Fuels 2010;24(12):6533–9. http://dx.doi.org/10.1021/ef100926v, URL https://pubs.acs.org/doi/10.1021/ef100926v.

[37] Encinar JM, González JF, Nogales-Delgado S. Thermogravimetry of the steam gasification of *Calluna vulgaris*: Kinetic study. Catalysts 2021;11(6):657. http: //dx.doi.org/10.3390/catal11060657, URL https://www.mdpi.com/2073-4344/ 11/6/657.

[38] Liu T, Fang Y, Wang Y. An experimental investigation into the gasification reactivity of chars prepared at high temperatures. Fuel 2008;87(4–5):460–6. http: //dx.doi.org/10.1016/j.fuel.2007.06.019, URL https://linkinghub.elsevier.com/retrieve/pii/S0016236107003158.

[39] Nzihou A, Stanmore B, Sharrock P. A review of catalysts for the gasification of biomass char, with some reference to coal. Energy 2013;58:305–17. http://dx.doi.org/10.1016/j.energy.2013.05.057, URL https://linkinghub.elsevier.com/retrieve/pii/S0360544213004787.

[40] Hognon C, Dupont C, Grateau M, Delrue F. Comparison of steam gasification reactivity of algal and lignocellulosic biomass: Influence of inorganic elements. Bioresour Technol 2014;164:347–53. http://dx.doi.org/10.1016/j.biortech.2014.04.111, URL https://linkinghub.elsevier.com/retrieve/pii/S0960852414006580.

[41] Dupont C, Nocquet T, Da Costa JA, Verne-Tournon C. Kinetic modelling of steam gasification of various woody biomass chars: Influence of inorganic elements. Bioresour Technol 2011;102(20):9743–8. http://dx.doi.org/10.1016/j.biortech.2011.07.016, URL https://linkinghub.elsevier.com/retrieve/pii/S0960852411009424.

[42] Prestipino M, Galvagno A, Karlström O, Brink A. Energy conversion of agricultural biomass char: Steam gasification kinetics. Energy 2018;161:1055–63. http://dx.doi.org/10.1016/j.energy.2018.07.205, URL https://linkinghub.elsevier.com/retrieve/pii/S0360544218315020.

[43] Bouraoui Z, Jeguirim M, Guizani C, Limousy L, Dupont C, Gadiou R. Thermogravimetric study on the influence of structural, textural and chemical properties of biomass chars on CO2 gasification reactivity. Energy 2015;88:703–10. http://dx.doi.org/10.1016/j.energy.2015.05.100, URL https://linkinghub.elsevier.com/retrieve/pii/S0360544215007021.

[44] Thengane SK, Gupta A, Mahajani SM. Co-gasification of high ash biomass and high ash coal in downdraft gasifier. Bioresour Technol 2019;273:159–68. http://dx.doi.org/10.1016/j.biortech.2018.11.007, URL https://linkinghub.elsevier.com/retrieve/pii/S096085241831527X.

[45] Huo W, Zhou Z, Chen X, Dai Z, Yu G. Study on CO2 gasification reactivity and physical characteristics of biomass, petroleum coke and coal chars. Bioresour Technol 2014;159:143–9. http://dx.doi.org/10.1016/j.biortech.2014.02.117, URL https://linkinghub.elsevier.com/retrieve/pii/S0960852414002880.

[46] Lin L, Strand M. Investigation of the intrinsic CO2 gasification kinetics of biomass char at medium to high temperatures. Appl Energy 2013;109:220–8. http://dx.doi.org/10.1016/j.apenergy.2013.04.027, URL https://linkinghub.elsevier.com/retrieve/pii/S0306261913003218.

[47] Lu G, Bai Y, Lv P, Wang J, Song X, Su W, et al. Ca-Si-Al interactions induced char structure and active site evolution during gasification–A comparative study based on different gasifying agent. Fuel 2022;316:123382. http://dx.doi.org/10.1016/j.fuel.2022.123382, URL https://linkinghub.elsevier.com/retrieve/pii/S0016236122002502.

[48] Zeng K, Minh DP, Gauthier D, Weiss-Hortala E, Nzihou A, Flamant G. The effect of temperature and heating rate on char properties obtained from solar pyrolysis of beech wood. Bioresour Technol 2015;182:114–9. http://dx.doi.org/10.1016/j.biortech.2015.01.112, URL https://linkinghub.elsevier.com/retrieve/pii/S0960852415001327.

[49] Rocca PAD, Cerrella EG, Bonelli PR, Cukierman AL. Pyrolysis of hardwoods residues: On kinetics and chars characterization. Biomass Bioenergy 1999;10.

[50] Blasi CD. Combustion and gasification rates of lignocellulosic chars. Prog Energy Combust Sci 2009;20.

[51] Tomaszewicz M, Tomaszewicz G, Sciazko M. Experimental study on kinetics of coal char–CO2 reaction by means of pressurized thermogravimetric analysis. J Therm Anal Calorim 2017;130(3):2315–30. http://dx.doi.org/10.1007/s10973-17-6538-3, URL http://link.springer.com/10.1007/s10973-017-6538-3.

[52] Kramb J, DeMartini N, Perander M, Moilanen A, Konttinen J. Modeling of the catalytic effects of potassium and calcium on spruce wood gasification in CO2. Crit Rev Environ Sci Technol 2017;148:50–9. http://dx.doi.org/10.1016/j.fuproc.2016.01.031, URL https://linkinghub.elsevier.com/retrieve/pii/S0378382016300303.

[53] Brown ME. Handbook of thermal analysis and calorimetry: Principles and practice. Elsevier; 1998, arXiv:33_3DBLGzMYC.

[54] Le C, Kolaczkowski S. Steam gasification of a refuse derived char: Reactivity and kinetics. Chem Eng Res Des 2015;102:389–98. http://dx.doi.org/10.1016/j.cherd.2015.07.004, URL https://linkinghub.elsevier.com/retrieve/pii/S026387621500249X.

[55] Adamon DGF, Fagbémi LA, Bensakhria A, Sanya EA. Comparison of kinetic models for carbon dioxide and steam gasification of rice husk char. Waste Biomass Valoris 2019;10(2):407–15. http://dx.doi.org/10.1007/s12649-017-0054-3, URL http://link.springer.com/10.1007/s12649-017-0054-3.

[56] Marquez-Montesinos F, Cordero T, Rodríguez-Mirasol J, Rodríguez JJ. CO2 and steam gasi®cation of a grapefruit skin char. 2002, p. 7.